

**Distribution of Bone Mineral Density(BMD) in Edentulous Mandible  
-A Measuring System of BMD Using Computed Radiography-**

Seiji TAKAOKA, Ken'ichi KOBAYASHI, Tsuguhisa KATOH\*, Shunsuke MINAKUCHI,  
Toshiaki SEKITA, Masanori NAGAO and Takehito SASAKI\*

Department of Geriatric Dentistry, Faculty of Dentistry, Tokyo Medical and Dental University

\*Department of Dental Radiology and Radiation Research, Faculty of Dentistry, Tokyo Medical and Dental University  
1-5-45, Yushima, Bunkyo-ku, Tokyo 113-8549 JAPAN

E-mail: s.takaoka.gero@dent.tmd.ac.jp

Commission V, Working Group 4

**KEY WORDS:** Computed Radiography, Bone Mineral Density, Mandible

**ABSTRACT**

In dental region, X-ray image provides useful information for denture or implant treatment, especially information on bone mineral density(BMD). The purpose of this study was to develop a *in vitro* measuring system for BMD using computed radiography(CR) and to make a distribution map of BMD in edentulous mandible with this system.

To reduce the structural noise on imaging plate, X-ray image with no object was subtracted from object image in optimum exposure condition. Each image of ninety sections cut from five edentulous mandible were divided into 64 elements. The mean BMD of every element was calculated and the BMD distribution map was made.

The system measured bone mineral content up to 1400mg/cm<sup>2</sup> and the detection limit was 11mg/cm<sup>2</sup>(2SD). Standard deviation of pixel value was reduced by factor 17 using the noise reduction technique. The accuracy of our BMD measuring system was 1.4%(relative error) and the reproducibility was 1.1%(CV).

In anterior region, between the mental foramina, the BMD of inferior cancellous bone was significantly higher than that of the lingual and labial side( $p < 0.001$ ). In posterior region, the BMD of buccal cancellous bone was significantly higher than that of the lingual side( $p < 0.001$ ). Greater individual variation of BMD was observed near mental foramen, and in incisor lingual and inferior cancellous bone.

Our BMD measuring system demonstrated excellent precision and reproducibility. BMD distribution varied near regions of muscle attachment and the mandibular canal. Deep placement of fixtures between the mental foramina in anterior region and placement into buccal cancellous bone within 24mm from the mental foramen in molar region may contribute to additional stability on endosseous implants.

**1. INTRODUCTION**

Bone quality and quantity is referred in many studies in osteoporosis, aging and other metabolic bone diseases. It is considered to be one of important factors for the prognosis of implant and denture prosthesis. Bone mineral density is one of the indices of the bone quality and reflects the degree of bone mineralization.

Many edentulous jaws are found among advanced ages. Previously, complete denture was only options available to restore masticating function for edentulous jaw. Recent advances in implant dentistry made implant retained dental prosthesis an alternative option.

For the those considering implant prosthesis, proper evaluation is necessary to determine wheater such treatment is appropriate in individual bases.

The relevance between bone quality and application of implant treatment was previously reported(Brånemark et al., 1977, Bass et al., 1991). However, the marginal BMD and its application for implant treatment is not well studied. 3-D distribution of BMD near planned implant placement site may be beneficial to know prior to implant placement. The previous studies about the BMD distribution in

edentulous mandible did not show the coordinates of distribution of measuring area, and are not precise enough for numerical comparison for BMDs among different areas.

BMD can be measured by 1) the scanning density of X-ray photo, 2)quantitative computed tomography, 3)dual energy X-ray absorptiometry. However, BMD measured by the technique 1) can be easily influenced by processing condition. The technique 2) has problem with spatial resolution and precision. The technique 3) it requires specialized devices.

The computed radiography(CR) system(Sonoda et al., 1983, Ogawa et al., 1995) uses an imaging plate(IP) in place of an usual X-ray film. The image data is obtained by scanning with laser beam. The image from CR is not affected by developing condition. The signal output is in proportion to X-ray dose. Digital radiography systems including CR are commonly characterized by a large dynamic range of the detector, an enough contrast with low dose of X-ray, and an availability of direct digital image processing. The CR image of 6 \* 4 inches has a high spatial resolution(2510 \* 2000 pixels, 0.1mm/pixel) and 8 bits gray scale. However, CR image has a noise mainly resulting from scattering X-ray and from IP structural noise. We are able to make a system for measuring bone mineral density using CR by controlling these noises. Therefore,

the objects of this study are 1)to develop the measuring system for bone mineral density using CR and 2)to create the distribution map of bone mineral density.

## 2. MATERIALS AND METHODS

### 2.1 Basic Theory

The placement of step wedge, object and water bath is shown in the Fig.1. We irradiate this water bath from a higher place. Let  $I_0$  be the intensity of an incident X-ray,  $I_1$  the one of an X-ray through reference step wedge and water,  $I_2$  the one of an X-ray through only water,  $I_3$  the one of an X-ray through bone and some soft tissue partition of object and water,  $I_4$  the one of X-ray through soft tissue partition of object and water,  $\mu_w$  the attenuation coefficient of water,  $\mu_r$  the one of reference step wedge,  $\mu_b$  the one of bone partition of object,  $\mu_p$  the one of soft tissue partition of object,  $x_w$  the depth of water,  $X_r$  the thickness of reference step wedge,  $X_{pb}$  the one of object,  $X_b$  the one of bone region of object. we have relations

reference step wedge:

$$\frac{I_1}{I_0} = \exp(-\mu_r X_r - \mu_w(x_w - X_r)) \quad (1)$$

water:

$$\frac{I_2}{I_0} = \exp(-\mu_w x_w) \quad (2)$$

bone region of object:

$$\frac{I_3}{I_0} = \exp(-\mu_b X_b - \mu_p(X_{pb} - X_b) - \mu_w(x_w - X_{pb})) \quad (3)$$

soft tissue region of object:

$$\frac{I_4}{I_0} = \exp(-\mu_p X_{pb} - \mu_w(x_w - X_{pb})) \quad (4)$$

Using Eqs. (1), (2), (3) and (4) we can derive

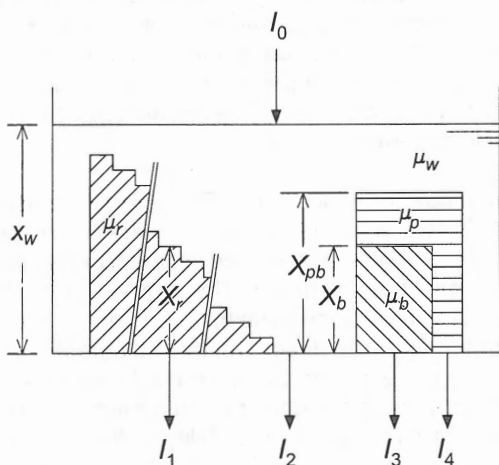


Fig. 1 The placement of reference step wedge(left side), object(right side) and water bath. The object is expressed as two partitions: a part equivalent to soft tissue(horizontal line area), a part equivalent to bone(slanting line area).

$$\log \frac{I_1}{I_2} = -(\mu_r - \mu_w) X_r \quad (5)$$

$$\log \frac{I_3}{I_4} = -(\mu_b - \mu_p) X_b \quad (6)$$

The attenuation rate of object in Eq.(6) can be expressed by a function of the step wedge thickness when the attenuation rate in Eq.(6) equals to it in Eq.(5).  $X_b$  is expressed as follows

$$X_{pb} = \frac{\mu_r - \mu_w}{\mu_b - \mu_p} X_r = \frac{\mu_r - \mu_w}{\mu_b - \mu_p} \rho_r X_r \quad (7)$$

$X_r$  is the reference material equivalent thickness(RMET) value. RMET value is the product of thickness and density  $\rho_r$ .  $X_r$  for practical use is divided by density, and is described by the thickness  $x_r$ (unit :  $\mu m$  ). The bone mineral density(BMD) is described by  $X_b$  divided by the thickness.

### 2.2 BMD Measuring System

This system was constructed with computed radiography system(Fuji FCR-7000, IP: Fuji ST-III) for X-ray image input device, image transmitting server(Fuji CR Station) and image processing workstation(Sun Ultra 1). Image data analysis was done using home made software on Solaris 2.5 with Motif 1.2.

Two custom-made step wedges were used in this

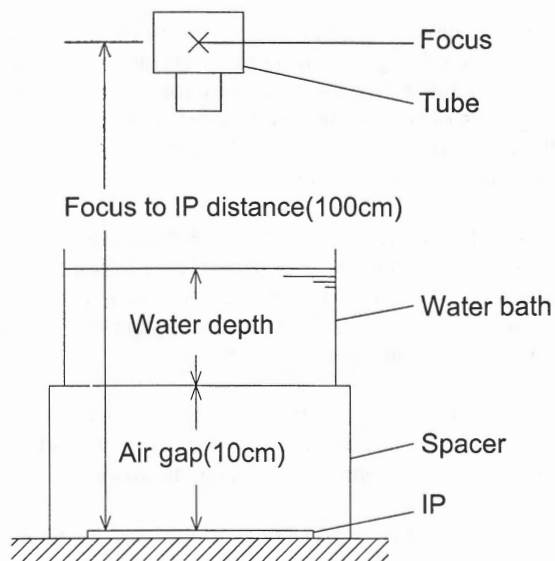


Fig. 2. Exposure placement and condition. Condition was IP to focus distance of 100cm, air gap of 10cm, tube voltage of 50kV and current of 32mAs, filter of CdS(51.1mg/cm<sub>2</sub>).

research; one for measuring bone mineral density with accuracy had 13 steps of 2mm thick, the other for examining precision had 15 steps of 1mm thick. These step wedges were made from polyester resin and mixture of  $\text{Ca}_3(\text{PO}_4)_2$  and  $\text{CaCO}_3$  (mole ratio 3:1). The exposure placement and condition were standardized; Focus-IP distance of 100cm, water depth of 3cm, air gap of 10cm, tube voltage of 50kV, tube current of 32mAs, filter of CdS(51.1mg/cm<sup>2</sup>)(Fig. 2).

The noise on X-ray image from the structural noise of IP was reduced by image subtraction. Fig. 3 schematically illustrates steps in subtraction.

The pixel value  $G_{ij}$ , where G is density of the pixel, and i, j are coordinates, was converted into RMET value  $R_{ij}$  by a cubic function curve after subtraction. Bone mineral density was obtained from this RMET value and the thickness of measuring area using Eq.(7).

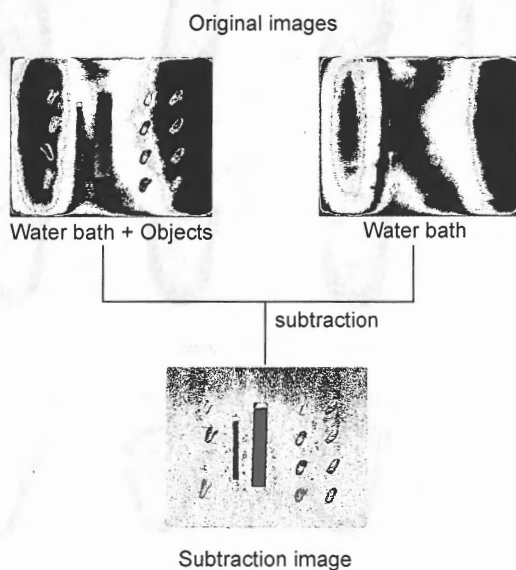
### 2.3 Measuring BMD of Mandible

The five edentulous mandibles were divided into body and rami of mandible. The bodies of mandible were embedded in polyester resin. The nine cross sections were cut from each lateral body of mandible; 90 sections were cut from five mandibles. Each section was manually ground to a thickness of 2-3mm. The sections were numbered from anterior to posterior; section 1 and 2 were incisor region, section 3,4 and 5 were premolar region, section 6 to 9 were molar region, section 4 took a position of the mental foramen.

The cross sectional X-ray image of each section was divided by the method as follows(Fig. 4).

#### A. In anterior region,

1. Select the top of alveolar process(R), the center of gravity



The noise from IP structural noise is reduced, and the signal gain is improved.

Fig. 3. Schematic representation of steps in the subtraction.

of section(G) and the farthest point from G on inferior border(F) as reference points.

2. The point of intersections of a straight line perpendicular to segment FG including G and the outline of section are  $P_L$  in lingual side and  $P_B$  in labial side. Each section from the mandible is divided into 4 regions by lines from G to every reference point. Each region is divided equally into 8 regions by straight lines including G. The intersections point of the dividing line and the outline were named  $P_i$  ( $i = 0, 1, \dots, 31$ ; starting from point R to labial side).
3. We can obtain 64 regions on each section by deciding the boundaries between cortical and cancellous region on 32 lines dividing each section.

#### B. In premolar and molar region,

1. Select points on mylohyoid muscle line(M) and external oblique ridge(E), the center of gravity of section(G) and the farthest point from G on inferior border(F) as reference points.
2. The point of intersection of the ray FG and the outline of section is U, the point of intersections of a straight line perpendicular to segment FG including G and the outline of section are  $P_L$  in lingual side and  $P_B$  in labial or buccal side. Each section from the mandible is divided into 6 regions by lines from G to every reference point. Each region upward on the segment  $P_L P_B$  is divided into quarters by straight lines including G, downward divided equally into 8 regions. The intersections point of the dividing line and the outline were named  $P_i$  ( $i = 0, 1, \dots, 31$ ; starting from point U to buccal side).
3. The same as A-3.

The thickness of each region was regulated by the thickness at a center of gravity in each region, the BMD in each region was measured.

The average cross-sectional shape was calculated from the polar coordinates of point  $P_i$ .

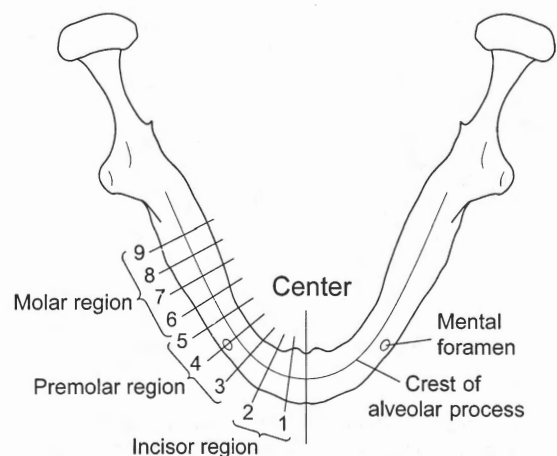


Fig. 4. Sectioning orientation.

Mental foramen was selected as a point of reference. Sections were cut from nine portions; mental foramen, 6, 12, 18mm anterior to and 6, 12, 18, 24mm posterior to it, crossing at right angle with a tangential line to crest of the alveolar ridge.

### 3. RESULTS

#### 3.1 BMD Measuring System

The standard deviation of the pixel value on X-ray image after subtraction was significantly reduced from 12.35 to 0.37 (Table 1). A significant linear, positive correlation was found between RMET value and bone mineral content (Fig. 6). The accuracy of measurement resulted 1.4% (relative error), and the reproducibility of BMC measurement resulted 1.1% (coefficient value).

#### 3.2 Distribution of BMD in Edentulous Mandible

The significant difference in BMD between the left and right side was not found. The distribution of BMD of edentulous mandible were expressed graphically in Fig. 7A. Fig. 7A shows cross sectional view. Fig. 7B and 7C shows panoramic view. Fig. 7C shows standard deviation (SD) of measurements. This SD represents the individual variation. The great individual variation was found; in cortical region - near the mental foramen and at the top of alveolar process in molar region, in cancellous region - at the lingual and the inferior border side in anterior region and at the labial side 6mm anterior to the mental foramen.

Fig. 8 shows the BMD in each side of cancellous bone. The BMD in lingual and inferior border side decreased from incisor to premolar to molar region. However the BMD in labial and buccal side showed no changes from incisor to section 8. At molar sections, the BMD in labial and buccal side was higher than the other regions. In all sides, the minimum value was found in section 2, moreover in section 4 at buccal side.

Fig. 9 shows the BMD in each side of cortical bone. The BMD in lingual and inferior border side decreased from incisor to molar region, however, the BMD in labial or buccal

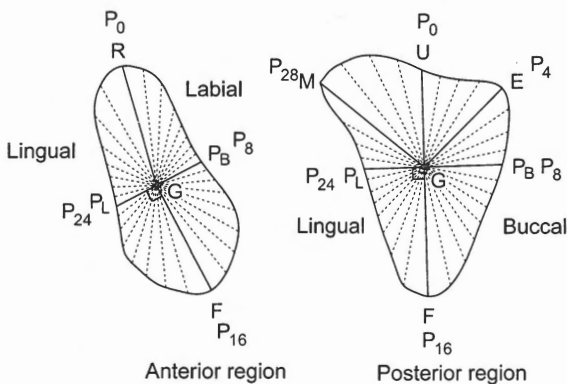


Fig. 5. Division of measuring region.

The left is a cross sectional view of anterior region, the right is of posterior region. R: crest of the alveolar process, M: the mylohyoid line, E: the external oblique line, G: the center of gravity of section, F: the farthest point from G on inferior border were reference points. The points were numbered from R to P<sub>B</sub> to F to P<sub>L</sub> to R in anterior region, from U to E to P<sub>B</sub> to F to P<sub>L</sub> to M to U in posterior region starting from P<sub>0</sub> to P<sub>31</sub>.

Table 1 Effect of subtraction

|                   | S.D.  | n  |
|-------------------|-------|----|
| Original image    | 12.35 | 37 |
| Subtraction image | 0.73  | 37 |

S.D.: Standard deviation of pixel value, n: Number of sample regions.

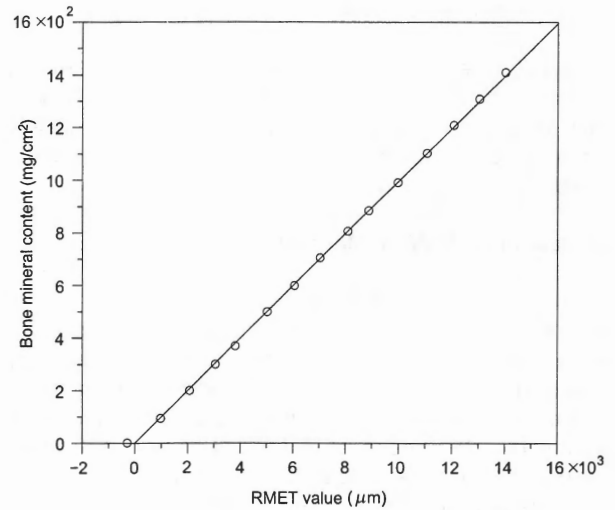


Fig. 6. Correlation between RMET value and bone mineral content.  $r=0.9999$ ,  $y=0.10x-3.69$ .

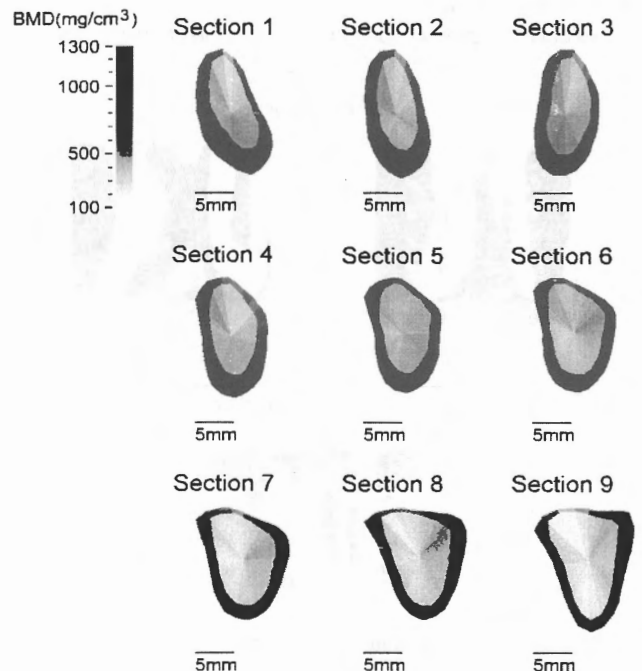


Fig. 7. Distribution of BMD in edentulous mandible; A: Cross sectional figure. Left side is lingual side, right side is labial/buccal side;

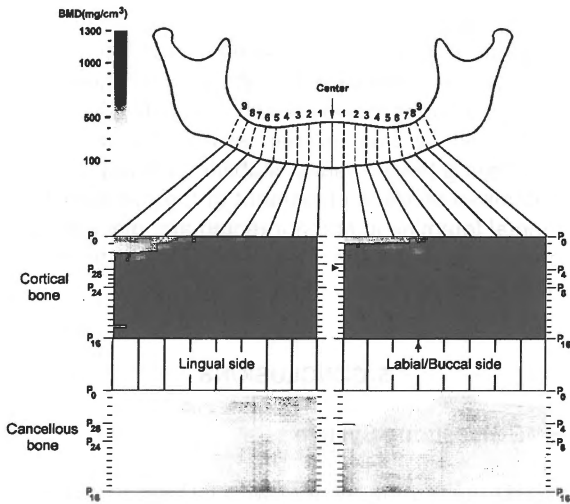


Fig. 7 B: Panoramic figure.

The upper figure shows the BMD distribution of cortical bone and the lower is one of cancellous bone. The symbol 'Δ' shows the place of mental foramen;

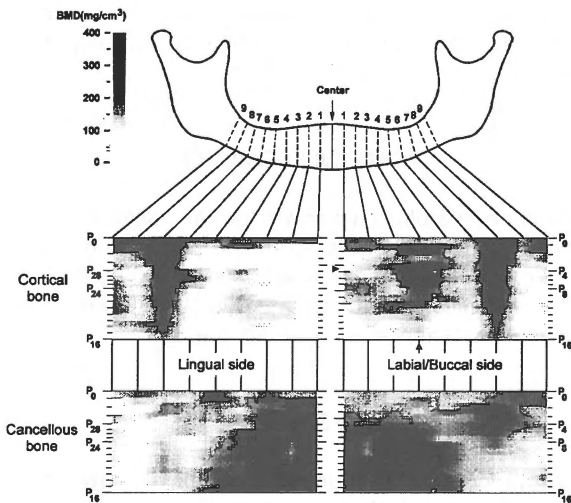


Fig. 7 C: Standard variation of measured BMD.

side increased. In all sides, the minimum value was found in section 2 and 4 similar to cancellous bone in labial or buccal side.

In anterior cancellous region, the BMD in inferior border side significantly showed higher than in alveolar side ( $p < 0.001$ ). In molar cancellous region, the BMD in buccal side was significantly higher than in lingual side ( $p < 0.001$ ). In cancellous and cortical bone, the BMD at the mylohyoid ridge was significantly higher than the surrounding areas ( $p < 0.001$ ). However the significant difference in BMD between at the external oblique ridge and at the surrounding areas was not found.

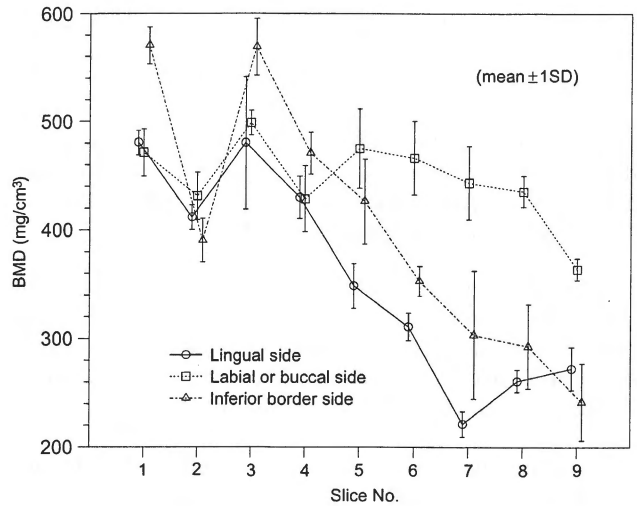


Fig. 8. Diagram of the BMD in each section of cancellous bone.

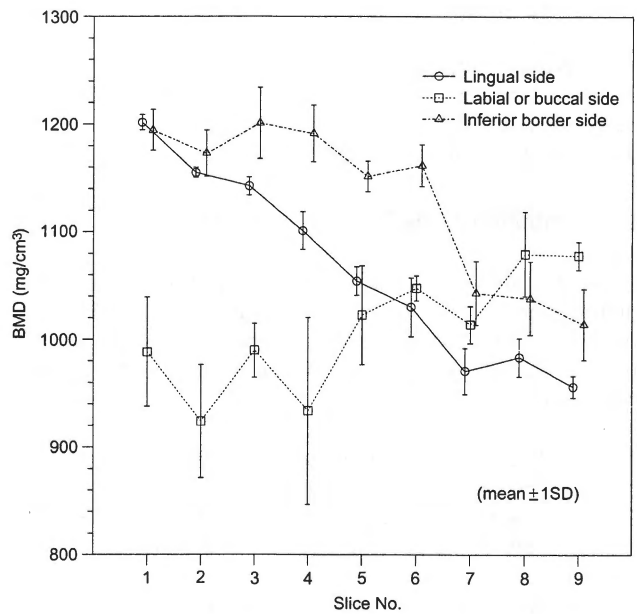


Fig. 9. Diagram of the BMD in each section of cortical bone.

## 4. DISCUSSION

### 4.1 BMD Measuring System

The noise in X-ray image with CR system consists of quantum noise and fixed noise. Quantum noise - X-ray photon noise and light photon noise - depends on exposure, and the size of noise is sufficiently smaller than that of signal when X-ray dose is enough. In this study, X-ray dose was sufficient for image formation. On the other hand, fixed noise - IP structural noise, electrical noise and quantization noise - is independent on exposure. IP structural noise is the most dominant among these fixed noises. The noise reduction method was for IP structural noise in our study. IP structural noise depends on not

uniformity of distribution of phosphor particles so that we used identical IP for exposure, and obtained reproducibility of noise by fixed relative position of IP.

The noise reduction is sufficient for the dynamic range of IP, because the standard deviation of the difference between mean pixel value and every pixel value was within 1 bit equal to the limit resolution of density.

The air gap reduces effect caused by scattered X-ray. In this study, the air gap of 10cm was enough for reducing noise from scattered X-ray. Furthermore, we used the water bath with 3 cm depth that is 32 \* 32 cm and that larger than IP in size to still more reduce noise from it.

The custom-made step wedge used in this study is made with  $\text{Ca}_3(\text{PO}_4)_2$  and  $\text{CaCO}_3$  (mole ratio 3 : 1). Since the element composition ( $\text{Ca}_{10}\text{P}_6\text{O}_{27}\text{C}$ ) is similar to the one of hydroxyapatite (HA) ( $\text{Ca}_{10}\text{P}_6\text{O}_{26}\text{H}_2$ ), the variation of mass attenuation coefficient with photon energy of this step wedge approximates to bone. This minimizes the measuring error.

The reproducibility of actual measurement system for BMD is approximately 1-3%(CV). The accuracy(1.4%) and reproducibility(1.1%) of our method are excellent, and satisfactory for measuring BMD.

#### 4.2 Distribution of BMD in Edentulous Mandible

Several quantitative analysis previously showed the BMD distribution in the mandible. Though, the approximate tendency of BMD variations is found from these result, they do not show detailed distribution of BMD in the mandible.

This study presents the new method that divides cortical and cancellous portions of the edentulous mandible into 64 cross-sectional parts. This allows the exact measurement at the precise position of the mandible.

The mandibles used for this study had various amount of the alveolar resorption. In general, intermediate amount of the alveolar ridge resorption was noted.

The BMD seems to change in accordance with places of muscle attachment and mental foramen, and with the changes of route of mandibular canal (Fig. 7A). The cortical bone at crest of the alveolar ridge in molar region seems to be largely affected by bone resorption (Fig. 7B).

Post-insertion stability and non-loading of the implant during the healing period are important factors for the success in implant treatment (Brånemark et al., 1977). Sufficient cortical bone is required to stabilize a newly placed implant (Misch, 1993). That is, an planned implant placement site in mandible should have an enough bone density to support fixture. Carter et al. (1976) shows that the compressive strength of bone is proportional to the square of the bone density. The BMD is evidently one of the important factors for stability. Therefore, the pre-examination of BMD near implant inserting site may be important for implant success.

This study showed that the BMD of lower region in anterior section was significantly higher than the BMD of upper region, and that the BMD in buccal side was higher than in lingual side at molar regions. Additionally, the BMD in labial and buccal side showed no changes from incisor to section 8. Considering these results, stability of implants can be best obtained by deep placement of the fixture between the mental foramina in anterior region and placement into buccal cancellous bone within 24mm from the mental foramen in molar region.

## 5. CONCLUSIONS

### 5.1 BMD Measuring System

The BMD measuring system with CR system provided sufficient accuracy(1.4%) and reproducibility(1.1%). The method for division of measuring region enabled the standardization of measuring position.

### 5.2 Distribution of BMD in Edentulous Mandible

The distribution of BMD showed adaptations to stress caused by muscles. For implant treatment to mandible in the lower jaw, deep installation of fixture between mental foramina in anterior region, installation to buccal cancellous bone in molar region may contribute to firm support to implant.

## ACKNOWLEDGMENTS

The authors gratefully acknowledge the assistance of Dr. Makoto Saigusa for helping in the preparation of our manuscripts. This research was supported by Grant-in-Aid for Scientific Research((C)(2)09671985)(The Ministry of Education, Science and Culture, Japan).

## REFERENCES

- Brånemark, P.I., Hansson, B.O., Adell, R., Breine, U., Lindstrom, J., Hallen, O. and Ohman, A., 1977. Osseointegrated implants in the treatment of the edentulous jaw. Experience from a 10-year period. *Scandinavian J. Plast. Reconstr. Surg., Suppl.*, 16, pp.1-132.
- Bass, S.L., Triplett, R.G., 1991. The effects of preoperative resorption and jaw anatomy on implant success. A report of 303 cases. *Clin. Oral Impl. Res.*, 2, pp.193-8.
- Ogawa, E., Arakawa, S., 1995. Quantitative analysis of imaging performance for computed radiography systems. *Proceedings of SPIE - the International Society for Optical Engineering*, 2432, pp.421-431.
- Sonoda, M., Takano, M., Miyahara, J. and Kato, H., 1983. Computed radiography utilizing scanning laser stimulated luminescence. *Radiology*, 148, pp.833-838.
- Misch, C.E., 1993. *Dentistry of Bone: Effect on Treatment Planning, Surgical Approach, and Healing*. Contemporary Implant Dentistry. Mosby, St. Louis, pp.469-485.
- Carter, D.R. and Hayes, W.C., 1976. Bone compressive strength: the influence of density and strain rate. *Science*,